

INDC International Nuclear Data Committee

NEUTRON DATA STANDARDS

Summary Report of the IAEA Consultants' Meeting

IAEA Headquarters, Vienna, Austria
12 – 16 October 2020
(virtual event)

A. Carlson
National Institute of Standards and Technology
Gaithersburg, MD, USA

V. Pronyaev
SC Rosatom (retired)
Moscow, Russia

D. Smith
Argonne National Laboratory (retired)
Coronado, CA, USA

R. Capote
International Atomic Energy Agency
Vienna, Austria

G. Schnabel
International Atomic Energy Agency
Vienna, Austria

June 2021

Selected INDC documents may be downloaded in electronic form from

<http://nds.iaea.org/publications>

or sent as an e-mail attachment.

Requests for hardcopy or e-mail transmittal should be directed to

NDS.Contact-Point@iaea.org

or to:

Nuclear Data Section
International Atomic Energy Agency
Vienna International Centre
PO Box 100
1400 Vienna
Austria

Printed by the IAEA in Austria

June 2021

NEUTRON DATA STANDARDS

Summary Report of the IAEA Consultants' Meeting

IAEA Headquarters, Vienna, Austria
12 – 16 October 2020
(virtual event)

A. Carlson
National Institute of Standards and Technology
Gaithersburg, MD, USA

V. Pronyaev
SC Rosatom (retired)
Moscow, Russia

D. Smith
Argonne National Laboratory (retired)
Coronado, CA, USA

R. Capote
International Atomic Energy Agency
Vienna, Austria

G. Schnabel
International Atomic Energy Agency
Vienna, Austria

ABSTRACT

The latest IAEA Neutron data standards were released in January 2018 (nds.iaea.org/standards/). This meeting was organized by the IAEA Nuclear Data Section to review the status of ongoing work for the development of the next version of the Neutron Data Standards that will be released within a few years. Due to a global pandemic (Covid-19), this meeting was conducted virtually during the week of 12-16 October 2020. There were 34 registered participants. Twenty-three talks were presented that addressed ongoing experimental and evaluation work for most of the Standard Cross Sections and Reference Cross Sections, as well as the development of updated evaluation methodologies, procedures, and codes. Presentations are available at nds.iaea.org/index-meeting-crp/CM-NDS-2020-10/. In the current work, priority is given and efforts are directed toward resolving existing discrepancies, establishing realistic uncertainties and correlations, and exploring the possibility of extending the applicable energy ranges of several important reactions in the suite of Standards and Reference Cross Sections through acquisition of new and/or improved data.

June 2021

Contents

1. INTRODUCTION.....	7
2. EXECUTIVE SUMMARY OF THE MEETING	7
3. PRESENTATION SUMMARIES.....	9
3.1. Recent work on neutron standards, A.D. Carlson (NIST, USA)	9
3.2. ${}^6\text{Li}(n,t)$ R-matrix fit of the CSNS Back-n data with RAC code, Chen Zhenpeng (TSU, China)....	9
3.3. ${}^{235}\text{U}(n,f)$ cross section from thermal to 170 keV, P. Finocchiaro (INFN, Italy)	9
3.4. Recent LANL work on reactions in the ${}^7\text{Li}$ System, G. Hale and M. Paris (LANL, USA).....	10
3.5. EDA R-matrix evaluations of NN and ${}^{17}\text{O}$ systems, M. Paris and G. Hale (LANL, USA)	10
3.6. ${}^{11}\text{B}$ Compound nucleus reaction: ${}^{10}\text{B}(n,Z)$ reactions, T. Massey (OU, USA).....	10
3.7. Reference prompt discrete γ -ray production and high energy fission cross sections, S. Simakov (KIT, Germany).....	11
3.8. Measurement of ${}^{235}\text{U}(n,f)$ cross section relative to ${}^1\text{H}(n,n)$ cross section in the energy range from 30 to 150 MeV at n_TOF, E. Pirovano (PTB, Germany)	11
3.9. Fission TPC cross section ratio results, L. Snyder (LLNL, USA).....	11
3.10. ${}^6\text{Li}(n,t)$ and ${}^{235}\text{U}(n,f)$ sub-thermal cross section measurements via an absolute cold neutron flux monitor, P. Mumm (NIST, USA).....	12
3.11. RPI measurements that can help improve cross section standards, Y. Danon (RPI, USA)	12
3.12. Carbon cross section, J. Vanhoy (USNA, USA)	13
3.13. Multigroup evaluation of the ${}^{235}\text{U}(n,f)$, ${}^{238}\text{U}(n,\gamma)$, ${}^{238}\text{U}(n,f)$ and ${}^{239}\text{Pu}(n,f)$ cross sections with the CONRAD code by using the GMA database: preliminary results, G. Noguere (CEA, France).....	13
3.14. On the thermal and resonance integrals as standards for neutron induced fission on major actinides, I. Duran (FICA-USC, Spain).....	15
3.15. Review of gold capture data, R. Reifarth (UF, Germany).....	15
3.16. ${}^{197}\text{Au}(n,\gamma)$ 30 keV Maxwellian: absolute integral measurements, J. Praena (UG, Spain).....	15
3.17. ${}^{238}\text{U}(n,\gamma)$ and ${}^{197}\text{Au}(n,\gamma)$ cross sections, S. Kopecky, C. Paradela and P. Schillebeeckx (EC-JRC, Geel).....	16
3.18. Status on AMS experiments: (1) ${}^{235}\text{U}(n,\gamma)$ at thermal and sub-thermal energies, (2) systematic difference between AMS & TOF, and (3) ${}^{235}\text{U}$ -PFNS– the threshold reaction ${}^{27}\text{Al}(n,2n)$, A. Wallner (HZDR, Germany)	17
3.19. Ad hoc approach for construction of USU covariances for GMA fit, V. Pronyaev (Russia) ...	18
3.20. Updating the ${}^{239}\text{Pu}(n,f)$ covariances in GMA with templates of expected uncertainties, D. Neudecker (LANL, USA).....	18
3.21. Variance analysis of the experimental data with prescribed statistical uncertainties, S.A. Badikov (Atomstandard, Russia).....	19
3.22. Prototype of a new Bayesian evaluation system – development and validation, G. Schnabel (IAEA)	19
3.23. Identifying physics reasons for outliers and systematic discrepancies in experimental ${}^{239}\text{Pu}(n,f)$ cross-section data using machine learning, D. Neudecker (LANL, USA)	20

4.	ACTION LIST	23
5.	RECOMMENDATIONS	25
	APPENDIX I: ADOPTED AGENDA.....	27
	APPENDIX II: PARTICIPANTS.....	29
	APPENDIX III: PRESENTATION LINKS.....	31

1. INTRODUCTION

The Meeting was opened by Arjan Koning, Head of the IAEA Nuclear Data Section. He welcomed all the participants to this important meeting of the Standards Data development effort, and continued to say that work was underway to make improvements in the current Standards Data library which had been released two years ago, in preparation of a new release in a few years. He emphasized the importance of meetings such as this as a platform to share information and coordinate the effort. Unfortunately, due to the Covid-19 global pandemic, the meeting had to be conducted virtually via WebEx instead of an in-person meeting at IAEA headquarters in Vienna. He thanked participants for agreeing to participate which, in many cases, involved getting up very early in the morning and, for others, staying up very late at night, and he said that the IAEA appreciated the effort and willingness to accommodate schedule disruptions in order to convene this meeting. The outcome, he was certain, would justify the sacrifices. Koning concluded by saying he hoped the next meeting could again take place in its usual setting, with participants convening at IAEA headquarters in Vienna.

Georg Schnabel, who served as IAEA meeting host, informed participants of the protocol required for such a meeting to proceed smoothly (video and audio connections, presentation uploading, muting to minimize acoustic feedback, etc.) and assisted participants to get properly connected virtually on Webex at the beginning of each meeting day.

Roberto Capote, Deputy Head of the IAEA Nuclear Data Section and meeting co-host, briefly summarized the work on previous standards, discussed issues regarding extension of the energy ranges, and emphasized all work done on unrecognized sources of uncertainties (USU) which resulted in a recently published paper in the Nuclear Data Sheets 163 (2020) 191-227. He also mentioned the extension of Pb, Bi, ^{235}U and ^{238}U fission cross-section references up to 1 GeV, new reference cross sections defined for $(n, n'\gamma)$ reactions, and the $^{252}\text{Cf}(\text{sf})$ and $^{235}\text{U}(\text{n}_{\text{th}}, \text{f})$ prompt fission neutron spectra (PFNS) which were also declared as reference spectra. These reference PFNS are available from the IRDFF-II library at nds.iaea.org/IRDFF/IRDFF-II_sp_ENDF.zip.

Allan Carlson was appointed Chair of the meeting, and Vladimir Pronyaev and Donald Smith agreed to serve as Rapporteurs. Due to potential legal considerations, it was decided that the meeting would not be audio-recorded although this feature is available in Webex. Links to presentations are given in Appendix III of this report.

2. EXECUTIVE SUMMARY OF THE MEETING

The focus of the meeting was to review the progress made toward the next evaluation of the neutron data standards. A very important contribution is measurements of neutron cross sections standards made at the China Spallation Neutron Source (CSNS). Work there includes measurements of the hydrogen scattering cross section by Jiang *et al.*, $^6\text{Li}(\text{n}, \text{t})$ angular distribution and cross section data by Bai *et al.*, $^{10}\text{B}(\text{n}, \alpha)$ and $^{10}\text{B}(\text{n}, \alpha_1)$ angular distribution and cross section measurements by Jiang *et al.*, and $^{238}\text{U}(\text{n}, \text{f})/^{235}\text{U}(\text{n}, \text{f})$ absolute cross section ratio measurements by Wen *et al.*. The close support from the CSNS collaboration we have had and anticipate will continue should allow improvements to be made in each of these standards.

In addition to the work at the CSNS, highlights of the meeting include:

H(n,n)

The anticipated extension of the hydrogen scattering standard to 200 MeV through the R-matrix analysis by Paris is important. The CSNS data and new measurements that have recently been completed by N. Kornilov *et al.* at Ohio University will be included in that analysis.

$^{10}\text{B}(\text{n}, \alpha)$, $^6\text{Li}(\text{n}, \text{t})$

The measurement of several cross sections having ^{11}B as a compound nucleus, by T. Massey *et al.*, combined with the CSNS and Finocchiaro $^6\text{Li}(\text{n}, \text{t})/^{10}\text{B}(\text{n}, \alpha)$ cross section ratio data, provide new input

for analysis of the $^{10}\text{B}(n,\alpha)$ and $^6\text{Li}(n,t)$ standards. Unfortunately, there is disagreement in the initial work reported at the meeting on the ^7Li system at higher energies by Chen Zhenpeng with the Hale and Paris analysis.

$^{\text{nat}}\text{C}$

Angular distribution work by Vanhoy was reported. Concerns were expressed concerning the difference between the last two evaluations of the integral $^{\text{nat}}\text{C}(n,n)$ cross section.

$\text{Au}(n,\gamma)$

The work by Praena and many others on the $^{197}\text{Au}(n,\gamma)$ 30 keV Maxwellian cross section substantiates the standards value.

Fission data

The measurement of the absolute $^{235}\text{U}(n,f)$ cross section by Pirovano *et al.* for 30 to 150 MeV (and higher) is the most recent measurement of this cross section. A NIST absolute measurement of the $^{235}\text{U}(n,f)$ cross section at a sub-thermal energy is underway. $^{235}\text{U}(n,f)$ cross section data were obtained in the $^6\text{Li}(n,t)$ and $^{10}\text{B}(n,\alpha)$ cross section work by Finocchiaro. It agrees with the standard in the standards energy region but from 9-18 keV neutron energy range it is lower by almost 5%. Danon has recently found that the $^{235}\text{U}(n,f)$ cross section from 0.01 eV to 3 keV is higher by 3% compared to the standards value. The TPC $^{239}\text{Pu}(n,f)/^{235}\text{U}(n,f)$ cross section ratio measurement with the TPC appears to be close to being finalized.

Reference cross sections

Status of the reference prompt discrete γ -ray production and high energy fission cross sections work was summarized by Simakov.

Thermal Constants

The importance of improving the $^{16}\text{O}(n,\alpha)$ cross section was emphasized since it affects ^{252}Cf nu-bar measurements when determined with Mn baths. A very preliminary value of ^{252}Cf nu-bar has been obtained by Hansell. McElroy and Croft (ORNL) are designing a new experiment to determine ^{252}Cf nu-bar to a high degree of accuracy. Noguere has produced a recent evaluation of the thermal constants using CONRAD.

$^{235}\text{U}(n,\gamma)$

$^{235}\text{U}(n,\gamma)$ results at thermal neutron energy were reported by Wallner.

Additional work on templates

Neudecker is considering templates work on the light element standards following her work done on fission cross sections.

USU

USU has had a large impact on the uncertainties of the standards. The evaluation of USU covariances based on the use of population statistics was considered. A detailed analysis based on uncertainty templates and outlier detection algorithms should be done before introducing USU. This may exclude to some extent the need for the use of USU in evaluations. If the introduction of USU is deemed necessary, statistical methods may be designed to incorporate the information of templates.

Machine learning

This concept could simplify evaluations of data. In its simplest form it involves training the “machine” to follow repetitive actions to reduce human effort. However, it is important to maintain the “human” element in obtaining quality evaluations.

Additional items

- The possibility of considering more energy intervals for normalizing data in addition to the 7.8 to 11 eV interval for $^{235}\text{U}(n,f)$ was discussed.
- Neutron energy standards: It was observed that on this issue little has been done since the 1991 NEANDC/INDC Nuclear Standards File work.

3. PRESENTATION SUMMARIES

Brief summaries of participants' presentations are given below, including their most important statements and conclusions. Full versions of the individual presentations are available in Appendix III of this report.

3.1. Recent work on neutron standards, A.D. Carlson (NIST, USA)

Significant work was reported at this meeting that encompassed contributions on experimental efforts, improvements in evaluation methods, studies of correlations, and USU, with a focus on extending the energy range of the standard cross sections and improving the reference data. Many of these experimental efforts could not be presented at this meeting. Thus, highlighted in this presentation was other work initiated, completed or proposed since the completion of the last evaluation of the neutron standards. Included were:

- H(n,n)H Angular Distribution Work at the China Spallation Neutron Source (CSNS), H. Jiang *et al.*, submitted to EPJA
- H(n,n)H Standard Angular Distribution Measurements at Ohio University, N. Kornilov *et al.*, Nucl. Sci. Eng. **194** (2020) 335.
- ${}^6\text{Li}(n,t)$ Measurements at LANL, L. Kirsch *et al.*, Nucl. Instrum. Methods Phys. Res., A **874** (2017) 57.
- ${}^6\text{Li}(n,t)$ Measurements at the CSNS, H. Bai *et al.*, Chin. Phys. C **44** (2020) 014003.
- ${}^6\text{Li}(n,t)$ Initiated Measurements at IRMM, K. Jansson *et al.*
- ${}^{10}\text{B}(n,a)$ and ${}^{10}\text{B}(n,a1)$ Initiated Measurements at GELINA, R. Bevilaqua *et al.*
- ${}^{10}\text{B}(n,a)$ and ${}^{10}\text{B}(n,a1)$ Measurements at CSNS, H. Jiang *et al.* Chin. Phys. C **43** (2019) 124002.
- ${}^{238}\text{U}(n,f)/{}^{235}\text{U}(n,f)$ Cross Section Ratio Absolute Measurements at CSNS, Wen *et al.* Ann. Nucl. Energy **140** (2020) 107301.
- ${}^{252}\text{Cf}$ nu-bar, Initiated Measurement by Hansell *et al.* at Drexel University as part of the PROSPECT collaboration
- ${}^{252}\text{Cf}$ nu-bar Proposed Measurement at ORNL, S. Croft *et al.*
- ${}^{235}\text{U}(n,f)$ Cross Section Measurements in the Axton Evaluation of the Thermal Constants. Impact of changes in the ${}^{234}\text{U}$ half-life on such measurements, including Deruytter's 1973 value.

3.2. ${}^6\text{Li}(n,t)$ R-matrix fit of the CSNS Back-n data with RAC code, Chen Zhenpeng (TSU, China)

For the presentation please refer to APPENDIX III – Presentation links.

3.3. ${}^{235}\text{U}(n,f)$ cross section from thermal to 170 keV, P. Finocchiaro (INFN, Italy)

The ${}^{235}\text{U}(n,f)$ cross section was measured at n_TOF relative to ${}^6\text{Li}(n,t)$ and ${}^{10}\text{B}(n,\alpha)$, with high resolution ($L = 183.49(2)\text{m}$) and in a wide energy range (25 meV–170 keV) with 1.5% systematic uncertainty, making use of a stack of six samples and six silicon detectors placed in the neutron beam. This allowed us to make a direct comparison of the yields of the ${}^{235}\text{U}(n,f)$ and of the two reference reactions under the same experimental conditions, and taking into account the forward/backward emission asymmetry. A hint of an anomaly in the 10–30 keV neutron energy range had been previously observed in other experiments, indicating a cross section systematically lower by several percent relative to major evaluations. The present results indicate that the cross section in the 9-18 keV neutron energy range is indeed overestimated by almost 5% in the recently released evaluated data files ENDF/B-VIII.0 and JEFF3.3, as a consequence of a 7% overestimate in a single GMA node in the IAEA reference file. Furthermore, these new high-resolution data confirm the existence of resonance-like structures in the keV neutron energy region. These results may lead to a reduction of the uncertainty in the 1–100 keV neutron energy region. Finally, from the present data, a value of $249.7 \pm 1.4(\text{stat}) \pm 0.94(\text{syst}) \text{ b} \cdot \text{eV}$ has been extracted for the cross section integral between 7.8 and 11 eV, confirming the value of $247.5 \pm 3 \text{ b} \cdot \text{eV}$ recently established as a standard. The ${}^{10}\text{B}/{}^6\text{Li}$ cross section ratio has been extracted and is in perfect agreement with the corresponding ratio from ENDF/B-VIII.0

3.4. Recent LANL work on reactions in the ${}^7\text{Li}$ System, G. Hale and M. Paris (LANL, USA)

We described an updated R-matrix analysis of the ${}^7\text{Li}$ system extending to 8 MeV neutron energy, which includes additional channels ($p+{}^6\text{He}$, $n+{}^6\text{Li}^{**}$) and several new data sets, including the extensive relative measurement of ${}^6\text{Li}(n,t){}^4\text{He}$ differential cross sections made recently by Bai *et al.* [1] at energies up to 3 MeV. This work was done as part of a major effort (CP2020) at Los Alamos this year to update the cross sections used in charged-particle transport.

Results of the fit were shown for the reactions ${}^4\text{He}(t,t){}^4\text{He}$, ${}^4\text{He}(t,n){}^6\text{Li}$, ${}^6\text{Li}(n,n){}^6\text{Li}$, ${}^6\text{Li}(n,t){}^4\text{He}$, ${}^6\text{Li}(n,p){}^6\text{He}$, and ${}^6\text{Li}(n,n_2){}^6\text{Li}^{**}$. Integrated cross sections for the latter two reactions measured by Presser *et al.* [2] were particularly useful to determine the nature of two interfering $3/2^-$ resonances in the 4-6 MeV region, which also affect the other reactions. The energy variation of the angular distributions for the ${}^6\text{Li}(n,t){}^4\text{He}$ reaction is well described by this analysis in the MeV region, and the integrated cross section there is quite different from the previous ENDF evaluation. A prominent peak around 6 MeV became a broader and more subtle feature, and these changes in the broad structure affect the cross section at lower energies within the present standards range ($E_n \leq 1$ MeV). An unresolved difference with the Bai data in the standards range is the value of the integrated cross section near the peak of the 240-keV resonance (3.54 b measured vs. 3.18 b calculated).

References:

- [1] H. Bai *et al.*, Measurement of the differential cross sections and angle-integrated cross sections of the ${}^6\text{Li}(n,t){}^4\text{He}$ reaction from 1.0 eV to 3.0 MeV at the CSNS Back-n neutron source, *Chinese Phys. C* **44** (2020) 013003.
- [2] G. Presser, R. Bass, and K. Krüger, The Reactions ${}^6\text{Li}(n,p){}^6\text{He}(0)$ and ${}^6\text{Li}(n,n){}^6\text{Li}(3.56)$, *Nucl. Phys. A* **131** (1969) 679-697.

3.5. EDA R-matrix evaluations of NN and ${}^{17}\text{O}$ systems, M. Paris and G. Hale (LANL, USA)

We give an overview of the nuclear data pipeline for evaluation of nuclear cross sections with the LANL code EDA. Single-experiment observables are defined as either unpolarized or polarized integrated and angular distributions for neutron and charged-particle incident projectiles for all processes (elastic, inelastic, reaction, break-up, etc.). Compilations of the single-experiment observables that couple to a given compound system are composed into compound-system data decks for all the relevant processes and observables. For example, the ${}^5\text{Li}$ compound system is composed of elastic (${}^3\text{He}(d,d){}^3\text{He}$ and ${}^4\text{He}(p,p){}^4\text{He}$) and reaction (${}^3\text{He}(d,p){}^4\text{He}$) data. The evaluation is carried out for all these data simultaneously using a single set of R-matrix parameters (including level energies and reduced widths) in a fully quantum-mechanical parametrization approach for the transition matrix. We applied this formalism to the NN and ${}^{17}\text{O}$ compound systems. For the NN system, we have extended the upper energy of the incident neutrons to 50 MeV. Comparisons of the existing fit for ${}^{13}\text{C}(a,n_0)$ are made to recent measurements from Febbraro *et al.* (PRL 125 062501 2020) for forward (zero degree) scattering; the predictions are of the correct order of magnitude but the lack of agreement in the shape indicates the need to take the current LANL/EDA evaluation to higher energy.

3.6. ${}^{11}\text{B}$ Compound nucleus reaction: ${}^{10}\text{B}(n,Z)$ reactions, T. Massey (OU, USA)

The experimental results for charge particles produced by neutrons on ${}^{10}\text{B}$ were presented. Four point angular distributions were reported for ${}^{10}\text{B}(n,\alpha){}^7\text{Li}(4.652)$, ${}^{10}\text{B}(n,\alpha){}^7\text{Li}(6.604)$, ${}^{10}\text{B}(n,p){}^{10}\text{Be}(g.s)$ and ${}^{10}\text{B}(n,t){}^8\text{Be}(g.s.)$. The sum of the differential cross sections for the ${}^{10}\text{B}(n,\alpha){}^7\text{Li}(g.s)$ and ${}^{10}\text{B}(n,\alpha){}^7\text{Li}(0.478)$ were also determined. Three point angular distributions for ${}^{10}\text{B}(n,d){}^9\text{Be}(g.s)$ were determined. Two points were obtained for ${}^{10}\text{B}(n,p){}^{10}\text{Be}(3.368)$ and ${}^{10}\text{B}(n,t){}^8\text{Be}(3.03)$. An R-Matrix analysis was done on these results to estimate the cross sections of these reactions. These cross sections estimated by the R-Matrix analysis were compared with the evaluated cross sections for ${}^{10}\text{B}(n,\alpha){}^7\text{Li}(g.s)$ and ${}^{10}\text{B}(n,\alpha){}^7\text{Li}(0.478)$.

3.7. Reference prompt discrete γ -ray production and high energy fission cross sections, S. Simakov (KIT, Germany)

In the period from 2017 to 2019, an evaluation of the prompt discrete γ -ray production cross sections was performed for reactions ${}^7\text{Li}(n,n')\gamma 478\text{keV}$ and ${}^{48}\text{Ti}(n,n')\gamma 948\text{keV}$ employing the GMA code. The former reaction was recommended for practical use as a reference at neutron energies 0.9 to 8.0 MeV with uncertainty 2% - 3%, the latter - from 2.8 to 16.0 MeV with uncertainty 3% - 4%. To extend the range of application, these two reactions could be combined with ${}^{10}\text{B}(n,\alpha_i)\gamma 478\text{keV}$ that is a standard from 1 MeV down to thermal energy with uncertainty 1%. When ${}^{10}\text{B}$ samples of various thicknesses are used, the self-shielding effect can be employed to generate gamma-ray calibration sources with variable effective neutron-energy thresholds in the range 1 to 100 keV, as can be seen from the slides that were presented at the meeting and are available for inspection through the links given in Appendix III.

The nuclear data needs for the reference discrete γ -ray production comprise the additional new measurements of (i) ${}^{48}\text{Ti}(n,n')\gamma 948\text{keV}$ cross section to reach uncertainty comparable with ${}^7\text{Li}(n,n')\gamma 478\text{keV}$ and (ii) angular distribution of the 948 keV γ -rays, since only controversial data exist at 14 MeV and since all evaluated libraries consider them as isotropic.

In 2017, the ${}^{238}\text{U}(n,f)$ reference cross section was re-evaluated between 200 and 1000 MeV using the LANSCE/LANL (n,f) data which became available only after the last evaluation in 2015. Additionally, several (p,f) cross sections (after their conversion into (n,f) with the help of the nuclear reaction code CEM03) were also included in the GMA fit.

New measurements of absolute (i.e., relative to n-p scattering) neutron induced fission cross sections for ${}^{235}\text{U}$, ${}^{238}\text{U}$, ${}^{239}\text{Pu}$ above 200 MeV are urgently needed. The (p,f) cross sections also will be helpful to establish the high energy (n,f) reference since they could be more easily and quickly measured.

The reference prompt discrete γ -ray production and high energy fission cross sections are made available on the IAEA Neutron Data Standards website as free text and ENDF6 formatted files. It was checked that the ENDF6 files are processable by the NJOY21 code.

3.8. Measurement of ${}^{235}\text{U}(n,f)$ cross section relative to ${}^1\text{H}(n,n)$ cross section in the energy range from 30 to 150 MeV at n_TOF, E. Pirovano (PTB, Germany)

One of the objectives of IAEA-NDS is the extension of the neutron energy range where the ${}^{235}\text{U}$ neutron-induced fission cross-section evaluation is a standard, to push its upper limit up to 1 GeV [INDC(NDS)-0681]. However, only two experimental datasets are available above 20 MeV, and none above 200 MeV. For this reason, a new experiment was carried out at n_TOF, the neutron time-of-flight facility of CERN, aimed at measuring the ${}^{235}\text{U}(n,f)$ cross section relative to the ${}^1\text{H}(n,n)$ cross section in the neutron energy range from 20 MeV to 1 GeV. The setup [EPJConf 239, 01008 (2020)] consisted of ten ${}^{235}\text{U}$ samples mounted in two reaction chambers, a Parallel Plate Avalanche Counter developed by IPN and a Parallel Plate Ionisation Chamber from PTB, and two polyethylene samples, which were all irradiated simultaneously. The protons emitted from the polyethylene radiators after elastic neutron scattering on hydrogen were counted using three particle telescopes placed outside the beam at the laboratory angles of 20 and 25 degrees. Two telescopes were designed by INFN and one by PTB.

In this contribution, the present state of the analysis for energies below 150 MeV was presented. The incident fluence on the uranium samples is reconstructed from the telescope data and the differential cross section of hydrogen using the transport codes MCNPX and Geant4, and the fission cross section is determined from the number of detected fission fragments. The calculation of the efficiency of the detectors is critical for the accuracy of the results. Systematic effects due e.g., to fission reaction anisotropy are still under study.

3.9. Fission TPC cross section ratio results, L. Snyder (LLNL, USA)

The fission TPC was designed for precision fission cross section ratio measurements. The high-fidelity 3D particle tracking data is used to conduct a detailed analysis of the uncertainty contributions. In this

contribution a brief overview of the instrument was presented. The results of the $^{238}\text{U}(n,f)/^{235}\text{U}(n,f)$ cross section ratio measurement published in [Phys. Rev C 97, 034618 (2018)] were reviewed and the preliminary status of the $^{239}\text{Pu}(n,f)/^{235}\text{U}(n,f)$ cross section ratio measurement was shown.

3.10. $^6\text{Li}(n,t)$ and $^{235}\text{U}(n,f)$ sub-thermal cross section measurements via an absolute cold neutron flux monitor, P. Mumm (NIST, USA)

The Alpha-Gamma apparatus at the National Institute of Standards and Technology utilizes the interaction of neutrons with a totally absorbing ^{10}B target to precisely measure the flux of a monochromatic cold (3.2 meV) neutron beam. This apparatus has previously been used to provide a calibration of the $^6\text{Li}(n,t)$ -based neutron flux monitor used in the NIST neutron lifetime experiment [1]. The earlier work reached a precision of slightly better than 0.1%, and demonstrated the technique as a novel way to measure other neutron interaction cross sections at sub-thermal energies. Of particular interest are measurements of ^{235}U neutron-induced fission and ^6Li neutron absorption cross sections where the technique can provide a systematically independent determination of these important quantities.

The cross section measurement requires knowledge of an areal density, a detector solid angle, and a charged particle count rate in addition to the neutron flux. It is carried out as follows: The flux monitor is placed upstream of the Alpha-Gamma apparatus which provides a precise measurement of the neutron flux. A thin and uniform neutron absorbing deposit on a silicon backing is mounted within the flux monitor and is viewed by four silicon detectors situated behind precision apertures that define precisely known solid angles. The total mass of neutron absorbing material on the deposit can be determined to high precision via sacrificial Isotope Dilution Mass Spectroscopy measurements of identical deposits. The total mass, combined with knowledge of the deposit profile obtained through ellipsometry or X-Ray fluorescence convolved with the neutron beam density obtained via conventional beam imaging techniques, allows for extraction of the needed areal density. Finally, the observed count rate in the silicon detectors, the areal density, and the solid angle can be combined to obtain the desired cross section after the application of several small systematic corrections. In the case of the ^{235}U measurement, the deposit is produced via evaporation of special reference material SRM-970 with a precisely known admixture of ^{234}U . Alpha counting of ^{234}U decays can then be used for an additional precise determination of the total ^{235}U mass. Expected precision on the cross sections are 0.2% - 0.3% for both $^{235}\text{U}(n,f)$ and $^6\text{Li}(n,t)$.

We have now carried out commissioning runs of both measurements. The results of these recent and ongoing measurements were presented, as well as plans for future operations.

References:

[1] A.T. Yue, et al, Metrologia **55** (2018) 460.

3.11. RPI measurements that can help improve cross section standards, Y. Danon (RPI, USA)

Several measurements previously performed at RPI that can be used to help improve the standards were discussed:

Accurate filtered beam total cross section measurements of carbon in the energy range from 24 keV to 1 MeV were discussed. In some of the measurement's energy range, the difference between ENDF-6.8 and 8.0 is larger than the uncertainty of the measured total cross section, and the experiment is in better agreement with ENDF-6.8, where a natural sample was used for the evaluation.

Quasi-differential scattering from a carbon sample was measured in the energy range from 0.5-20 MeV. The experimental data at different angles were plotted as a function of time-of-flight (or equivalent incident neutron energy) and compared to a detailed simulation of the experiment. Some differences between the measurement and the ENDF-7.1 and 8.0 evaluations were noted. Overall, simulations with the ENDF-8.0 evaluation are in better agreement with the data.

A simultaneous measurement of U-235 fission and capture yields in the energy range from 0.01-2.5 keV was discussed and compared to the ENDF-7.1 and 8.0 evaluations. The fission experiment was normalized to the U-235 thermal value of the evaluation it was compared with. The experimental data

were grouped to wide energy bins to compare with the evaluations. The fission yield is in agreement with the ENDF-8.0 and 7.1 evaluations, within the 2% accuracy of the measurement, over the entire energy range. Comparison of the capture yield to ENDF-7.1 and 8.0 shows difference of up to 7% in different energy ranges, most notably at 0.0253-9.4 eV with C/E=1.06 and at 7.8-11 eV with C/E=1.07. Such differences were not observed with ENDF-7.1.

A measurement of Cf-252 prompt fission neutron spectrum using the gamma tagging method was presented. Within its uncertainty, this measurement supports the standard PFNS spectrum up to about 6 MeV. In the energy range of 6-8 MeV the experiment is lower than the evaluation and it was suggested that additional experimental data with lower uncertainty is needed.

3.12. Carbon cross section, J. Vanhoy (USNA, USA)

Elastic and inelastic neutron scattering cross sections were performed on natural carbon samples. Fifty (n,n') differential cross sections were measured at 32 incident neutron energies between 0.3 and 8.0 MeV.

Angle-integrated elastic cross sections are consistent with ENDF8.0 values, with the exception of the region 3.2 to 4.0 MeV where our results are 3% higher. In the 3.4 to 3.6 MeV region our angular distributions are slightly lower at forward angles and slight greater at backward angles than the ENDF8.0 calculations; however, our measurements are consistent with measured data by other research groups. First through fourth order elastic scattering Legendre coefficients are consistent with ENDF8.0 values.

Inelastic scattering was measured at 7 incident energies between 5.6 and 7.0 MeV. Angle-integrated cross sections track the 1969 Perey and ENDF8.0 values very well. Angular distributions trend similar to the ENDF8.0 calculations. The research group intends to measure more (n,n₁) cross sections over the next three years to guide improvements in resonance parameters.

3.13. Multigroup evaluation of the $^{235}\text{U}(n,f)$, $^{238}\text{U}(n,\gamma)$, $^{238}\text{U}(n,f)$ and $^{239}\text{Pu}(n,f)$ cross sections with the CONRAD code by using the GMA database: preliminary results, G. Noguere (CEA, France)

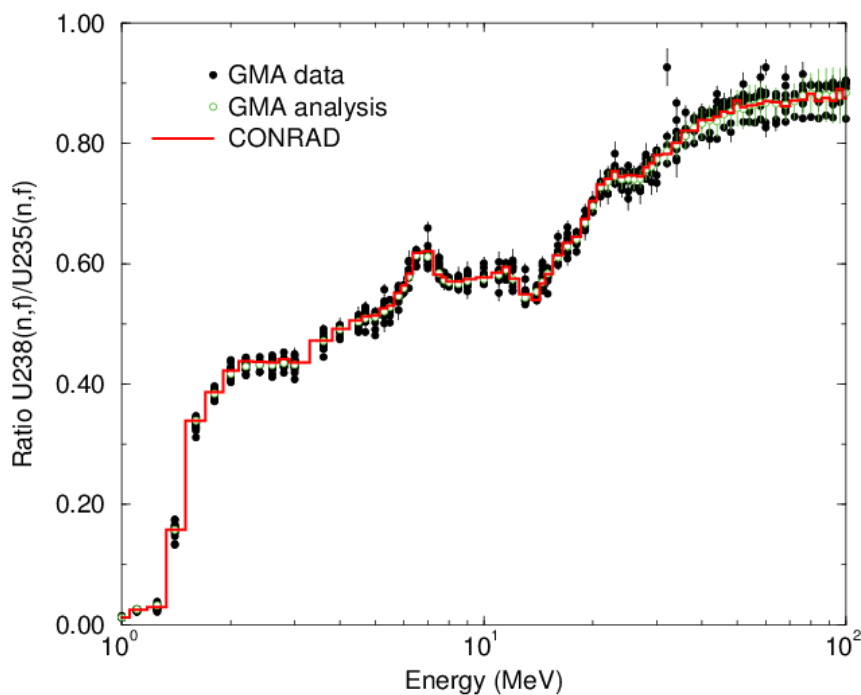


FIG. 1. Comparison of the experimental values of the ratios $^{238}\text{U}(n,f)/^{235}\text{U}(n,f)$ available in the GMA database and the results provided by the GMA analysis [4] and the CONRAD code.

The evaluation of the neutron standards is historically performed with the GMA code [1]. An independent analysis is in progress with the CONRAD code [2], developed at the CEA of Cadarache.

The originality of the present approach is to include in the analysis the neutron cross section data available in the GMA database together with the Thermal Neutron Constants (TNC) of ^{233}U , ^{235}U , ^{239}Pu and ^{241}Pu listed by Axton in Ref. [3]. The data sets can be divided into seven types of data, namely “Absolute“, “Shape“, “EDA-RAC“ (for ^{10}B and ^6Li), “Theory“ (for ^{10}B and ^6Li), “Spectrum average“ (for ^{235}U and ^{239}Pu), “RRR evaluation“ (for ^{238}U capture cross section from Derrien) and “TNC“ (from Axton and new data). We have used 161 energy groups from thermal to 200 MeV (instead of 163 in the original GMA analysis) because $E=0.235$ MeV and $E=0.980$ MeV are missing for $^{239}\text{Pu}(n,f)$ and $^{238}\text{U}(n,\gamma)$, respectively. A total of about 6500 data points and 1000 free parameters are included in the CONRAD calculations.

Figure 1 compares the experimental values of the ratios $^{238}\text{U}(n,f)/^{235}\text{U}(n,f)$ available in the GMA database and the results provided by the GMA analysis [4] and the CONRAD code. As a first step, the CONRAD calculations only use the variances of the GMA data. The full correlation information will be included in the second step. A maximum of about 2% of differences is observed between the results provided by the GMA analysis and the CONRAD calculations. Part of such differences can be attributed to the covariances.

A closer inspection of all the results in terms of C/E (Fig. 2) shows local differences, which are well above 2%. In some cases, the obtained differences correspond to GMA data with large uncertainties. This result indicates that part of the GMA database has to be carefully revisited, having in mind that some older data sets became obsolete, when new accurate measurements are introduced in the analysis.

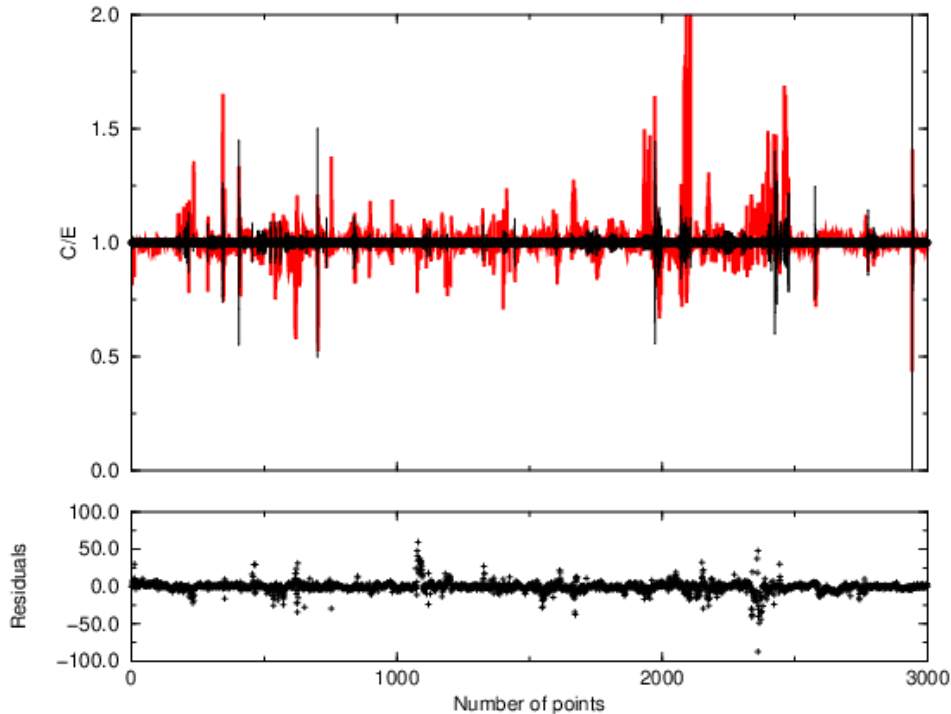


FIG. 2: Ratio (in red) between the CONRAD results (C) and the “Absolute” GMA data. The black line corresponds to the relative uncertainties of the GMA data.

The present work suggests converting the GMA database into a readable format to avoid user-dependent mistakes. Then, new mathematical approaches are needed (i) to test the reliability of the data (using well defined rejection criteria), (ii) to replace the “Theory” data type by constraints in the fitting procedure and (iii) to revisit the “node” description (extrapolation to the nodes with prior theoretical

calculations, multi-group description ...). A broader discussion is also recommended to explore new fitting theories beyond the naïve Bayesian technique routinely used in nuclear data.

References:

- [1] W.P. Poenitz and S.E. Aumeier, The simultaneous evaluation of the standards and other cross sections of importance for technology, ANL/NDM-139, 1997.
- [2] P. Archier *et al.*, CONRAD evaluation code: development, status and perspectives, Nucl. Data Sheets **118** (2014) 488.
- [3] E.J. Axton, Evaluation of the thermal constants of ^{233}U , ^{235}U , ^{239}Pu and ^{241}Pu , and the fission neutron yield of ^{252}Cf , JRC-Geel report, GE/PH/01/86, 1986.
- [4] A.D. Carlson *et al.*, Nucl. Data Sheets **148** (2018) 143.

3.14. On the thermal and resonance integrals as standards for neutron induced fission on major actinides, I. Duran (FICA-USC, Spain)

Significant improvements in the evaluations of neutron-induced fission cross-section datasets will require that the input values of physical quantities that are incorporated be more accurate than those currently employed for ND Standard or Reference purposes.

The aim of this contribution is to propose as reference or standard quantities some new integral data for the fissile major actinides - namely ^{233}U , ^{235}U , ^{239}Pu and ^{241}Pu – in the thermal region and in the low energy region of the resolved resonance. These integral data should help to improve both the normalization and the energy calibration of the experimental datasets from high-resolution high-accuracy experiments. In addition, it is proposed to adopt some “fiducial points” defined as the E_n value at the peak of the (n,f) cross section for a few isotopes having resonances with large cross sections and very small widths.

Concerning the energy integral intervals used for (n,f) reaction reference, four intervals have been identified for ^{235}U , and two for each of the other three fissile isotopes. For both $^6\text{Li}(n,t)$ and $^{10}\text{B}(n,\alpha)$ reactions it is proposed to define integral intervals around 1 eV, where the shape of the cross section as a function of E_n is well known to fit a straight-line in log-log coordinates. Further work should be done to define the limits of such intervals.

Concerning the fiducial points, the following resonance peaks are proposed as good candidates to be included in an IAEA reference file:

- 8.773(3) eV resonance peak of the $^5\text{U}(n,f)$ reaction, as this isotope is widely used as monitor.
- 5.903(8) keV resonance peak of the $^{27}\text{Al}(n,\text{tot})$ reaction, as aluminum is a common material used at every experimental setup and this very narrow peak is found as black filter.
- 4.895(5) eV resonance peak of the $^{197}\text{Au}(n,\gamma)$ reaction, as natural gold is monoisotopic and it is very often used as thin-foil black-filter.

3.15. Review of gold capture data, R. Reifarth (UF, Germany)

For presentation please refer to APPENDIX III – Presentation links.

3.16. $^{197}\text{Au}(n,\gamma)$ 30 keV Maxwellian: absolute integral measurements, J. Praena (UG, Spain)

The motivation of this work arose in 2012 from the discrepancy between the absolute integral measurements of Ratynski and Käppeler (RK) of the Maxwellian Average Cross Section (MACS) of $^{197}\text{Au}(n,\gamma)$ at $kT=30$ keV, average value (582 ± 9) mb, and time-of-flight values in facilities such as Gelina (EU), (613 ± 9) mb, and n_TOF (CERN), (611 ± 22) mb. We obtain the MACS at 30 keV, (625 ± 15) mb, with absolute integral measurements based on the production of ^7Be and the activation of ^{197}Au to ^{198}Au . Also, we applied corrections to the RK analysis which provide a new value of 622 mb, making the RK experiment still very useful [1].

Our experiments used two different neutron fields. First, we used the RK field produced by the ${}^7\text{Li}(p,n)$ reaction at $E_p=1912$ keV. The RK field resembles a *quasi*-Maxwellian Neutron Spectrum at $kT=25$ keV (so-called QMNS-25). The difference with RK is that we used flat Au samples instead of semi-spherical Au samples. A first experiment provided a value of (626 ± 17) mb [1]. Recently, we carried out three new experiments that yielded the values (629 ± 14) mb, (634 ± 13) mb and (625 ± 13) mb. The corrections in the analysis are [1]: 1) spectrum correction from QMNS-25 to Maxwellian at 30 keV, performed by RK but with the Macklin Au cross-section; 2) neutron scattering correction on the target, performed by RK in a different way; 3) flat sample correction, not needed for RK. Also, we checked the QMNS-25 field by means of the TOF technique at CNA [2]. As the second activation method, we used a neutron field resembling a Maxwellian Neutron Spectrum at 30 keV (MNS-30). It is based on shaping a 3.66 MeV proton beam to a Gaussian distribution close to the threshold of the ${}^7\text{Li}(p,n)$ reaction by means of an Aluminium foil which it traverses before it collides with the Lithium target [3]. We obtained a value of (612 ± 17) mb [4]. Thus, the average value of the five activations is (625 ± 15) mb. The Tandem accelerator at CNA (Spain) was carefully calibrated before our experiments providing an uncertainty lower than 1 keV in the proton energy [3].

We reanalysed the RK value considering [1]: 1) neutron scattering on the setup with MCNPX, not available in 1988, we obtained up to 5% instead of 1.8% by RK with the activation of small Au foils located upstream from the neutron target; 2) spectrum correction from 0.5-3 keV, not taken into account by RK because of the Macklin Au cross-section, this provides 2% correction; 3) ${}^{198}\text{Au}$ half-life, RK used 2.62 d meanwhile at present it is 2.6941 d, which provides +10 mb. With these corrections, the RK value changes from 582 to 622 mb.

Conclusions: We provide an average value of (625 ± 15) mb with five absolute integral measurements with flat samples, four with QMNS-25 and one with MNS-30 field. The evaluation of neutron standards, (620 ± 11) mb, could slightly underestimate the MACS of ${}^{197}\text{Au}(n,\gamma)$ at $kT=30$ keV. The RK value with new corrections, not possible in 1988, is very useful. Finally, semi-spherical samples were only used in RK. Flat samples were used in MACS measurements of several elements. Flat sample correction depends on the cross-section of the element being measured. We studied cases with $\sigma(E)\sim E^{-a}$ for $a=0.4-0.8$ showing that corrections from 2 to 4% should be applied, i.e. ${}^{13}\text{C}$ [5]. Thus, some MACS measurements by activation should be reanalyzed with a flat sample correction included.

References:

- [1] P. Jiménez-Bonilla and J. Praena. Proceedings of Science PoS (NIC XIII Conf.) 102 (2014).
- [2] M. Macías, B. Fernández and J. Praena. Rad. Physics and Chemistry **168** (2020) 108538.
- [3] J. Praena, P. Mastinu *et al.*, Nucl. Inst. and Meth. in Physics Res. A **727** (2013) 1–6.
- [4] P. Jiménez-Bonilla, J. Praena *et al.* NPA VII (2015) Conf., J. Phys.: Conf. Ser. 940 (2018) 012044.
- [5] P. Jiménez-Bonilla, J. Praena *et al.* Nuclei in the Cosmos XV (2018), Proceedings in Physics 219.

3.17. ${}^{238}\text{U}(n,\gamma)$ and ${}^{197}\text{Au}(n,\gamma)$ cross sections, S. Kopecky, C. Paradela and P. Schillebeeckx (EC-JRC, Geel)

The status of the cross sections for ${}^{197}\text{Au}(n,\gamma)$ and ${}^{238}\text{U}(n,\gamma)$ in the unresolved resonance region (URR) was reviewed. In addition, the experimental procedures that were applied to produce experimental data at the time-of-flight facility GELINA for an evaluation of these cross section in the URR were discussed [1,2].

Capture cross section measurements were carried out by applying the total energy detection principle in combination with the pulse height weighting technique. The weighting functions (WF) were determined by Monte Carlo simulations which were validated by experiment [3].

In the calculation of the weighting functions, the effect of gamma-ray transport in the sample and the discrimination level of the detection system were taken into account.

Bias effects on the normalization due to nuclear data and sample properties were minimized due to the use of an internal saturated resonance. Fixed black resonance filters were used to reduce bias effects due to the impact of the sample properties on the background level [4]. The uncertainties of the normalization and background corrections were evaluated based on results of dedicated experiments.

The averaged capture yields were corrected for self-shielding and multiple interaction events to produce averaged capture cross sections. To produce a full evaluation in the URR that can be used for reactor calculations including self-shielding, average resonance parameters were derived by applying the Hauser-Feshbach approach with width fluctuations. These parameters were derived by a least squares adjustment to average capture and total cross sections [1,5].

The status of the $^{197}\text{Au}(n,\gamma)$ and $^{238}\text{U}(n,\gamma)$ cross sections recommended by the neutron standards project [6] was discussed by comparing them with recent data obtained at GELINA [1,2], LANSCE [7] and n_TOF [8,9,10]. This comparison illustrated the good agreement between the cross sections recommended by the standards project and the experimental data that are available in the literature. However, it also illustrated the limitations of the recommended cross sections which do not reproduce fluctuations due to remaining resonance structures. These structures are clearly observed by comparing the average capture cross sections derived from measurements at different flight path stations at GELINA. These limitations are primarily due to the energy binning that is presently used for the analysis with GMA. The use of the $^{197}\text{Au}(n,\gamma)$ and $^{238}\text{U}(n,\gamma)$ cross sections as neutron reference cross sections in the unresolved resonance region could be improved by adapting the energy binning to remaining structures.

References:

- [1] C. Massimi *et al.*, Eur. Phys. J. A 50 (2014) 124.
- [2] H.I. Kim *et al.*, Eur. Phys. J. A 52 (2016) 170.
- [3] A. Borella *et al.*, Nucl. Instr. Meth. A 577 (2007) 626.
- [4] P. Schillebeeckx *et al.*, Nucl. Data Sheets 113 (2012) 3054.
- [5] I. Sirakov *et al.*, Eur. Phys. J. A 53 (2017) 199.
- [6] A.D. Carlson *et al.*, Nucl. Data Sheets 110 (2009) 3215.
- [7] J.L. Ullmann *et al.*, Phys. Rev. C 89 (2014) 034603.
- [8] C. Lederer *et al.*, Phys. Rev. C 83 (2011) 034608.
- [9] F. Mingrone *et al.*, Phys. Rev. C 95 (2017) 034604.
- [10] T. Wright *et al.*, Phys. Rev. C 96 (2017) 064601.

3.18. Status on AMS experiments: (1) $^{235}\text{U}(n,\gamma)$ at thermal and sub-thermal energies, (2) systematic difference between AMS & TOF, and (3) ^{235}U -PFNS – the threshold reaction $^{27}\text{Al}(n,2n)$, A. Wallner (HZDR, Germany)

(1) We presented a new campaign to measure the neutron capture cross section of ^{235}U for thermal and cold energies using accelerator mass spectrometry (AMS). The goal of this project is to achieve an uncertainty of order 3% for the cross section value. Neutron irradiations have been performed at BR-1 (Mol, Belgium) with thermal neutrons, as well as at FRM-II, Munich with cold neutrons (2 activations), and at ILL, Grenoble with very cold neutrons. These three different activations will allow exploration of the energy-dependence of the cross section in the sub-thermal to thermal energy range. Natural Uranium-oxide samples are used which enables the study in parallel of the capture cross section of ^{238}U in the same sample. AMS directly counts the reaction products, ^{236}U and ^{239}Pu (decay product of $^{238}\text{U}(n,\gamma)^{239}\text{U}$). Part of the AMS measurements are finished. Still pending is the measurement of the ILL sample, and as well a cross calibration of reference samples used for ^{236}U and ^{239}Pu counting, to new reference materials ordered from JRC Geel.

(2) We studied the two reactions $^{35}\text{Cl}(n,\gamma)$ and $^{54}\text{Fe}(n,\gamma)$ for the Maxwellian-Average Cross Sections (MACS) at ca. 25 keV, which is of interest to nuclear astrophysics. Previous measurements using AMS for a number of reactions with the same geometry show a systematic difference of the MACS to data obtained from complementary TOF measurements. Here, an independent neutron irradiation and the use of different AMS facilities should clarify whether some systematic uncertainties plague the AMS method for these reactions [1]. The experiments are finished and a publication of these results is in progress.

(3) The measurements of a number of threshold reactions in the $^{235}\text{U}(n_{\text{th}},f)$ reference neutron field aim at validating the PFNS high-energy tail of the neutron spectrum. Within an international collaboration, an experiment at ILL Grenoble utilized cold neutrons to bombard a ^{235}U sample where the emitted prompt fission neutrons irradiated a stack of different monitor foils thereby enabling mapping of the high energy neutron distribution. In particular, we focused on the threshold reaction $^{27}\text{Al}(n,2n)^{26}\text{Al}$, which has its threshold at 13.5 MeV. Thus, this reaction is sensitive only to the highest neutron energies in the PFNS spectrum. Accelerator mass spectrometry was used again to count the number of produced ^{26}Al atoms for three different Al monitor foils. Despite a shorter neutron irradiation campaign than foreseen, leading to a significantly lower neutron fluence on the samples, we have successfully measured the ^{26}Al content in the various samples. Discussion is ongoing regarding which level of accuracy is needed in the AMS measurements, as these measurements, being close to the measurement background level, are very time consuming. A successful result however is already provided with the existing data.

References:

- [1] Z. Slavkovská, A. Wallner, R. Reifarth, S. Pavetich, B. Brückner, K. Al-Khasawneh, S. Merchel, M. Volkandt, M. Weigand, Investigation of $^{54}\text{Fe}(n,\gamma)^{55}\text{Fe}$ and $^{35}\text{Cl}(n,\gamma)^{36}\text{Cl}$ reaction cross sections at keV energies by Accelerator Mass Spectrometry, EPJ Web of Conferences **232** (2020) 02005.

3.19. Ad hoc approach for construction of USU covariances for GMA fit, V. Pronyaev (Russia)

The long-standing problem of too small uncertainties of the neutron cross section standards is discussed. An ad hoc method is proposed for evaluation of the covariance matrix of unrecognized sources of uncertainties (USU) contributing in the final covariances of the evaluated data. Sample statistics of biases of experimental data relative to the posterior "true" evaluation, taking account of known (recognized) uncertainties, is used for estimation of USU covariances.

It is concluded that a) the analysis and assignment of components of uncertainties to the results of measurements using templates for given methods of measurements, b) inclusion of known and hidden correlations between components of uncertainties in the results of measurements done with the same method, and c) statistically justified approaches to deal with outliers, enables the generation of more realistic evaluation of uncertainties in the standards fit without the need to introduce USU.

3.20. Updating the $^{239}\text{Pu}(n,f)$ covariances in GMA with templates of expected uncertainties, D. Neudecker (LANL, USA)

This talk was about how templates of expected measurement uncertainties can be used to update covariances in the GMA database such that missing, but known, uncertainties in GMA can be detected and filled in. Two issues were raised by the community that might lead to underestimated GMA evaluated uncertainties: (a) not all pertinent uncertainties for single data sets are considered in GMA, and (b) correlations between uncertainties of the same and different experiments were missing. By accounting for those known, but missing, uncertainties and correlations in GMA via the template, we can reduce the need for quantifying USU. While quantifying USU is essential to give a realistic degree of evaluated uncertainties for the standards, the use of unknown uncertainties should be reduced to the absolute minimum needed. The templates are one way to do this.

Templates of uncertainties expected in specific measurement types were recently developed for (n,f) cross section in D. Neudecker *et al.*, Nucl. Data Sheets 264, 228 (2020). One aim of these templates is to aid in identifying (1) missing or suspiciously low uncertainties and (2) missing correlations between uncertainties of the same and different experiments, when estimating covariances for experimental data employed in evaluations. These templates also provide realistic estimates of standard deviations and correlations for a particular uncertainty source and measurement type. This information can be used by evaluators if it is not supplied by the experimenters. If applied to all covariances in GMA, this information allows for a more comprehensive uncertainty analysis across all measurements in the database, thus, reducing the need for USU.

In the talk, I presented how an (n,f) template of uncertainties was applied to improving covariances of $^{239}\text{Pu}(n,f)$ cross-section measurements in the GMA database. The evaluated uncertainties obtained after updating the covariances in the database by means of the template increase compared to their original values (up to 30%). The evaluated mean values change significantly enough to impact the simulation of selected Pu metal fast criticality values by more than 70 pcm.

However, we should not only confine this update of GMA covariances to $^{239}\text{Pu}(n,f)$ cross sections as many different observables (e.g., $^{235}\text{U}(n,f)$, $^{10}\text{B}(n,\alpha)$, $^6\text{Li}(n,t)$, $^{238}\text{U}(n,f)$, and $^{238}\text{U}(n,\gamma)$) in GMA are interconnected by ratio measurements. Hence, updating uncertainties of data sets of any of these observables can potentially impact the $^{239}\text{Pu}(n,f)$ cross section and vice versa. Uncertainties for all measurements of these linked physical observables have to be updated to arrive at more realistic evaluated uncertainties for all observables evaluated with GMA, which in turn leads to changes in the cross section.

It was discussed at the meeting that the changes in GMA for the $^{239}\text{Pu}(n,f)$ cross sections can be checked by the committee and will likely be adopted. It was also discussed that the (n,f) template will be applied to $^{235}\text{U}(n,f)$ and $^{238}\text{U}(n,f)$ cross sections next and then extended to other observables. Templates for other observables are currently being established by a CSEWG initiative.

3.21. Variance analysis of the experimental data with prescribed statistical uncertainties, S.A. Badikov (Atomstandard, Russia)

Variance analysis is an iterative analysis of the parameters of distributions. In particular, this entails treating the distributions of deviations of the model function from the experimental data grouped in a special way.

In the general case, no input information on the uncertainties of the experimental data is considered in the variance analysis. As shown by R. Capote *et al.*, “USU in the Experimental Nuclear Data”, Nuclear Data Sheets, 163, p. 191 (2020) and some other publications, the variance analysis provides primary estimates for the statistical and systematic uncertainties, as well as correlations of systematic errors. Any additional reliable input experimental information could improve the results of the analysis.

In the example considered, the variance analysis with the prescribed statistical experimental uncertainties yields larger uncertainties of the evaluated values of the model function compared to the result of the general case. This effect can be explained by a more realistic balance between statistical (given) and systematic (estimated) components of the experimental uncertainty.

3.22. Prototype of a new Bayesian evaluation system – development and validation, G. Schnabel (IAEA)

W. Poenitz was a strong advocate of using Bayesian inference to combine the information of multiple datasets for the evaluation of neutron cross sections [1]. Since then, the GMA code developed by Poenitz and later extended by Smith and Pronyaev [2] (and renamed to GMAP) was successfully applied to the evaluation of neutron data standards, the latest version being documented in [3]. The complexity of the GMAP code due to the mathematics involved and the use of Fortran-77, especially the frequent use of goto-statements, makes it difficult to improve upon methodology and to remove constraints on input data without potentially breaking existing functionality. An implementation of an evaluation system functionally equivalent to GMAP in Python would make future improvements of methodology and the addition of features easier and less error prone. The code logic can be formulated at a higher level of abstraction which improves readability and extensibility. A first translation of GMAP from Fortran-77 to Python was successfully undertaken, and its equivalence to the Fortran version verified by comparing the outputs of the Fortran and Python code for a comprehensive collection of input data. Their produced outputs have been found to be equivalent within a relative numerical tolerance smaller than $5 \cdot 10^{-5}$ which is a strong indication for their functional equivalence. The remaining discrepancy is quite compatible with the hypothesis that Python uses double precision whereas the Fortran version performs some operations with single precision. Indeed, the numerical discrepancy can be significantly decreased by promoting a few constants to double precision in the Fortran code. Both the Fortran and

Python GMAP version are available on the IAEA-NDS GitHub account. This presentation also discussed a potential need to update the mathematical methodology employed in the GMAP code to account for an energy-dependent USU (=unrecognized source of uncertainty) component, and it showed preliminary results of an extension of GLS that can account for energy-dependent USU. The potential existence of USU (=unrecognized source of uncertainty) components, and their impact and possible treatment in evaluations, has already been discussed in detail in [4].

References:

- [1] W.P. Poenitz, Data interpretation, objective evaluation procedures and mathematical techniques for the evaluation of energy-dependent ratio, shape and cross section data, Proc. of the Conf. on Nuclear Data Evaluation Methods and Procedures, Brookhaven National Lab., Sep. 22-25 1980, IAEA Report INDC(USA)-85, 1981, pp. 249 - 285.
- [2] D.L. Smith and V.G. Pronyaev, Update of GMA Code to Solve the PPP Problem (Technically), IAEA Vienna, 25-Nov-2003, Private Communication.
- [3] A.D. Carlson et al, Evaluation of the Neutron Data Standards, Nuclear Data Sheets 148 (2018) 1.
- [4] R. Capote et al, Unrecognized Sources of Uncertainty (USU) in Experimental Nuclear Data, Nuclear Data Sheets 163 (2020) 191-227.

3.23. Identifying physics reasons for outliers and systematic discrepancies in experimental $^{239}\text{Pu}(n,f)$ cross-section data using machine learning, D. Neudecker (LANL, USA)

This talk was about how machine learning (ML) methods can be used to identify physics reasons for outliers and systematic discrepancies in experimental data in the GMA database. This talk was again geared towards trying to minimize the need for USU. USU stems from discrepancies evident between several data sets in the GMA database that are not represented by their respective uncertainties (i.e., overlapping uncertainties) nor are understood with respect to their underlying physics reason. It is essential that we try to understand the underlying physics biases in the data in order to either add uncertainties or correct the data. If we fail to do so, we will assess the spread of the data as USU and this uncertainty will remain as a minimum, no matter what high-precision measurements will be added to the database in the future.

One complication in understanding what part of a measurement is driving the discrepant behavior (i.e., what part of the analysis or equipment could lead to bias) is that most nuclear-data measurements are composite in nature, i.e., the reported values (cross section, $\bar{\nu}$, PFNS, etc.) are extracted by combining several measurements (count rate, number of atoms in the sample, flux....) and corrections. They have different attributes (features in ML language, e.g.: detector type) related to these measurements and corrections. To find the reason for outliers with expert knowledge can be tricky if there are too many common features across many experiments, but ML methods are designed to find trends in a large amount of data.

To this end, we studied which features of 24 $^{239}\text{Pu}(n,f)$ cross-section data sets of GMA are related to outliers in B. Whewell *et al.*, NIMA Vol. 978, 164305 (2020). We studied 37 feature categories per measurement with about 100 values across the 24 measurements. For instance, methods to determine the background, sample backing material, or impurities in the sample, are explicitly taken into account in the ML process. To this end, outliers in the experimental data are identified with a modified version of the Hybrid Robust Support Vector Machine with about 50% overlap between outliers found by the GMA procedure and the algorithm chosen here. In a second step, two very different machine learning methods (logistic regression with elastic net regularization and random forest regression with SHAP feature importance metric) are used to highlight measurement features that are common among many of the outlying data points. The ML algorithms agree with regards to the most important features related to outliers and accepted data which indicates a certain robustness of the algorithms. These results can give us confidence that, indeed, the algorithms can find reasonable trends in a lower amount of data than available in GMA. Hence, it is realistic that we can apply these algorithms in a stable manner to GMA data. It is also shown that the results are not only stable but also plausible. More specifically, the

ML algorithms find features related to outliers and accepted data that are indeed expected by experts. But it also finds unexpected ones, showing us again that ML might find things that experts can miss due to the large amount of data. In short: ML algorithms can be applied in a stable manner (i.e., enough data) and reliably (giving plausible results) to highlight potential shortcomings in the experimental data that could lead to a physics understanding of discrepancies. It is always up to the physicist to decide if the results are helpful. ML augments but does not replace expert judgment. Hence, these algorithms can provide important information to identify potential reasons for USU. One issue is that we need the features for the data, an undertaking which is time-intensive. A collaboration with SG-50 might help. In order to aid the standards, SG50 will extend their aim to include standards observables.

4. ACTION LIST

No.	Action	Participant(s)	Due by
1	Provide a prescription for users who need H(n,n) cross section data above 20 MeV (possibly the latest Arndt's evaluation).	Hale, Paris	June 2021
2	Include Komilov's 14.9 MeV data for H(n,n) angular distributions in the analysis if not already there.	Paris	June 2021
3	Contact CSNS about the possibility of extending H(n,n) measurements above 52 MeV. Can absolute data be obtained?	Carlson, Capote	May 2021
4	Suggest that the CSNS group redo ${}^6\text{Li}(n,t)$ and ${}^{10}\text{B}(n,\alpha)$ measurements as a ratio to avoid using ${}^{235}\text{U}(n,f)$ for fluence measurement.	Carlson, Capote	June 2021
5	Add n_TOF data for ${}^6\text{Li}(n,t)$ to ${}^{10}\text{B}(n,\alpha)$ ratio measurements to GMA data base.	Schnabel, Pronyaev	June 2021
6.	Include Bai <i>et al.</i> and Massey <i>et al.</i> data for boron in the R-matrix fit.	Paris, Chen	June 2021
7	Prepare a request for the HPRL concerning charged particle measurements of alpha particles incident on ${}^6\text{Li}$ and tritons on ${}^7\text{Li}$ leading to formation and decay of the ${}^{11}\text{B}$ compound nucleus system. Also include in that request measurements of total neutron cross sections for materials such as boron.	Hale, Carlson, Capote	June 2021
8	Contact Vanhoy-Kentucky University group to see if angular distribution/total cross section measurements could be made on an enriched ${}^{13}\text{C}$ sample.	Carlson	June 2021
9	Incorporate the carbon total and angular distribution measurements of Vanhoy <i>et al.</i> into the evaluation. Suggest additional energies where angular distributions should be measured by Vanhoy. Investigate the worsening agreement of the most recent total elastic evaluation with data of Danon (it now differs by about 1% for the total cross section). Investigate the angular distribution data at RPI that indicate differences with both recent standards evaluations at back angles (at 156 degrees) in the standards energy region.	Paris, Hale	December 2021
10	Up to now, only 8 angular distributions for the neutron energy range 1.48 – 3.8 MeV are compiled in EXFOR for ${}^{12}\text{C}(n,el)$ from about 50 angular distributions in the energy range 0.65 – 7.96 MeV that have been measured. No inelastic scattering and gamma-production data are in EXFOR. Send these data for compilation and have all available numerical data compiled.	Vanhoy, NNDC Otsuka	December 2021
11	Examine the issue related to use of n_TOF data in GMA Standards analyses, including channels binning and data reduction to the nodes for evaluation.	Pronyaev, Finocchiaro	June 2021
12	Add CSNS ${}^{238}\text{U}(n,f)/{}^{235}\text{U}(n,f)$ cross section ratio data by Wen to the evaluation. Add the absolute ${}^{235}\text{U}(n,f)$ cross section by Pirovano <i>et al.</i> for 30 to 150 MeV (and higher) to the evaluation. Add the NIST absolute measurement of the ${}^{235}\text{U}(n,f)$ cross section at a sub-thermal energy to the evaluation (if extrapolation to the thermal value will be possible). Add the Finocchiaro ${}^{235}\text{U}(n,f)$ cross section data obtained relative to the ${}^6\text{Li}(n,t)$ and ${}^{10}\text{B}(n,\alpha)$ cross sections.	Schnabel, Neudecker, Pronyaev, Pirovano	When data will be available

<i>No.</i>	<i>Action</i>	<i>Participant(s)</i>	<i>Due by</i>
13	Add the latest TPC values for $^{238}\text{U}(n,f)$ to the evaluation.	Schnabel, Neudecker, Pronyaev, Snyder	June 2021
14	Add the latest TPC values for $^{239}\text{Pu}(n,f)$ to the evaluation.	Schnabel, Neudecker, Pronyaev, Snyder	June 2021
15	Prepare and send to the IAEA/NDS a limited list of narrow resonances proposed for use as neutron energy calibration standards; and neutron energy ranges for the fission cross section in the resonance region of different actinides proposed to be used as integral cross section standards.	Duran	June 2021
16	The use of more detailed energy bins should be proposed and discussed. For example, 10 equidistant nodes in log scale (lethargy) per decade could be used below 100 keV, and additional nodes could be provided near thresholds (e.g., for $^{238}\text{U}(n,f)$) and for regions of noticeably varying cross sections. The influence of these changes on the combined fit of the data then should be investigated.	Schnabel, Pronyaev, Neudecker	June 2021
17	Study the problem of high-resolution TOF data reduction to the nodes (weighted or unweighted averaging to wider bins and use of grouped or line-interpolated point presentation of data).	Schnabel, Pronyaev	December 2021
18	Proposed work at ORNL for nu-bar ^{252}Cf should be included when finalized. Nu-bar results by Hansell for ^{252}Cf should be included when finalized.	Schnabel, Pronyaev, Noguere	When data will be available
19	Continue work on the templates. Important work could be done on light element standards. Check experiments with charged-particles (same compound nucleus) that often have very high weight in R-Matrix evaluations. Are those weights justifiable?	Neudecker, Paris	December 2021
20	Study the origin of discrepancies between $^{238}\text{U}(n,\gamma)$ cross sections measured by activation method relative to $^{197}\text{Au}(n,\gamma)$ and the method involving gamma-ray detection in TOF measurements used in the Standards database.	Pronyaev, Schillebeeckx	December 2021
21	Come to a conclusion about the possibility of using the machine learning approach for searching for outliers and correcting for them.	Neudecker	June 2023
22	Undertake the extended UQ for U-235(n,f) measurements	Neudecker	June 2022

5. RECOMMENDATIONS

It is recommended:

- (1) to limit all further coding work on GMA(P) to producing a robust version in Python that yields values that agree with the current Fortran version for diverse input data from the GMA database, but introduces no new features. This version can be used for evaluation purposes until such time that a more modern code is developed that eliminates the widely acknowledged limitations of GMA(P) that were necessitated by limitations of computer technology for small computers 40 years ago. The new code should be given an entirely new name to avoid confusion with GMA(P). Furthermore, a companion code should be developed to translate the GMA input format to a new, backward compatible data format with enhanced capability for dealing with various uncertainty types, including USU and complete correlation information, and that this new format should be the one used by the new code;
- (2) to continue work on updating the GMA experimental database for covariances using the templates approach developed at LANL to assign and revise uncertainties. Effort should be expended to correct errors and problems in the GMA database found during work leading to the ND2019 publication “New fit of thermal neutron constants (TNC) for $^{233,235}\text{U}$, $^{239,241}\text{Pu}$ and $^{252}\text{Cf}(\text{sf})$: Microscopic vs. Maxwellian data”;
- (3) that the IAEA/NDS prepare and send a support letter to the members of WPEC SG-50 group encouraging their involvement in the analysis of the GMA data sets for $^{235}\text{U}(\text{n},\text{f})$, $^{238}\text{U}(\text{n},\text{f})$, $^{238}\text{U}(\text{n},\gamma)$, $^{197}\text{Au}(\text{n},\gamma)$ reaction cross sections, their ratios, and ratios to $^6\text{Li}(\text{n},\text{t})$, $^{10}\text{B}(\text{n},\alpha)$ $^{10}\text{B}(\text{n},\alpha,\gamma)$ reaction cross sections for the uncertainties quantification process based on the prepared template;
- (4) to use revised data structures for GMA thermal constants. The present input data structure creates a misunderstanding in many cases. This can be done together with rewriting GMA in a modern programming language. The experimental data for thermal values (constants) and their correlations could be introduced directly in the GMA fit and not in the form of pre-evaluated constants with cross correlations as it is done now;
- (5) that the latest experimental data for the thermal constants be used for the fits by both CONRAD and GMA, in the manner suggested in the final sentence of recommendation (4);
- (6) to extend the data analysis and evaluation for $\text{H}(\text{n},\text{n})$ by Paris as high in energy as is reasonably possible – at least to 200 MeV;
- (7) to use both R-matrix codes EDA and RAC for the evaluation of $^6\text{Li}(\text{n},\text{t})$, $^{10}\text{B}(\text{n},\alpha)$ and $^{10}\text{B}(\text{n},\alpha_1)$ standard reactions. The fits should be made with the same experimental data in the energy range up to 2 MeV.
- (8) to study the use of I1 and I3 integrals of the measured neutron-induced fission cross sections near the thermal region (I1) and near first resonances (I3) of fissile targets to define reference (normalization) integrals for those measurements that do not reach the thermal point. I3/I1 ratio could be also defined as a reference ratio, which is similar to the ratio $\text{I3}/\sigma_0$, with σ_0 being the thermal fission cross section.
The following energy boundaries were recommended for I1 and I3 integrals:
Integral I1: from 20 up to 60 meV for all targets (which is equivalent to the thermal cross section)
Integral I3, with different boundaries for each target:
U-235: 7.8 eV up to 11 eV (already used as reference)
U-233: 8.1 eV up to 14.7 eV
Pu-239: 9 eV up to 20 eV
Pu-241: 11.7 eV up to 14.7 eV
- (9) to study whether the ratios of fission cross-section integrals relative to the integral of Li and B cross sections in the energy region near the thermal point can also be defined as reference ratios, as these are experimentally measured quantities with low uncertainty.

APPENDIX I: ADOPTED AGENDA

Monday, 12 October

13:50 Technical setup and checks

14:00 Opening (IAEA)

A. Koning, R. Capote, G. Schnabel (IAEA)

**14:10 Election of Chairman and Rapporteur
Adoption of the Agenda**

14:20 Introduction

R. Capote

14:35 Participants' Presentations

14:35 Recent work on neutron standards, A. Carlson (NIST, USA)

15:10 ${}^6\text{Li}(n,t)$ R matrix fit of the CSNS Back-n data with RAC code, Chen Zhenpeng (TSU, China)

15:35 ${}^{235}\text{U}(n,f)$ cross section from thermal to 170 keV, Paolo Finocchiaro (INFN, Italy)

16:05 Break

16:15 Recent LANL work on reactions in the ${}^7\text{Li}$ system, G. Hale (LANL, USA)

16:40 EDA R-matrix evaluations of NN and ${}^{17}\text{O}$ systems, M. Paris (LANL, USA)

17:05 ${}^{11}\text{B}$ compound nucleus reactions: ${}^{10}\text{B}(n,Z)$ reactions, T. Massey (OU, USA)

17:30 Discussion

Tuesday, 13 October

14:00 Participants' Presentations (cont'd)

14:00 Reference prompt discrete γ -ray production and high energy fission cross sections, S. Simakov (KIT, Germany)

14:30 Measurement of ${}^{235}\text{U}(n,f)$ relative to ${}^1\text{H}(n,n)$ in the energy range from 30 to 150 MeV at n_TOF, E. Pirovano (PTB, Germany)

14:55 FissionTPC cross section ratio results, L. Snyder (LLNL, USA)

15:25 Break

15:35 ${}^6\text{Li}(n,t)$ and ${}^{235}\text{U}(n,f)$ sub-thermal measurements via an absolute cold neutron flux monitor, P. Mumm (NIST, USA)

16:00 RPI measurements that can help improve cross section standards, Y. Danon (RPI, USA)

16:30 Carbon scattering cross section, J. Vanhoy (USNA, USA)

17:00 Discussion

Wednesday, 14 October

14:00 Participants' Presentations (cont'd)

- 14:00 Multigroup evaluation of the $^{235}\text{U}(n,f)$, $^{238}\text{U}(n,\gamma)$, $^{238}\text{U}(n,f)$ and $^{239}\text{Pu}(n,f)$ cross sections with the CONRAD code by using the GMA database: preliminary results, G. Noguere (CEA, France)
- 14:30 Review of gold capture data, R. Reifarh (UF, Germany)
- 15:00 $^{197}\text{Au}(n,\gamma)$ 30 keV Maxwellian: absolute integral measurements, J. Praena (UG, Spain)
- 15:25 On the thermal and resonance integrals as standards for neutron induced fission on major actinides, I. Duran (USC, Spain)

15:50 Break

- 16:00 $^{238}\text{U}(n,\gamma)$ and $^{197}\text{Au}(n,\gamma)$ cross sections, P. Schillebeeckx (EC-JRC Geel)
- 16:30 Status on AMS experiments: (1) $^{235}\text{U}(n,\gamma)$ at thermal and sub-thermal energies, (2) systematic differences between AMS & TOF, and (3) ^{235}U -PFNS – the threshold reaction $^{27}\text{Al}(n,2n)$, A. Wallner (HZDR)

16:55 Discussion

Thursday, 15 October

14:00 Participants' Presentations (cont'd)

- 14:00 Ad hoc approach for construction of USU covariances for GMA fit, V. Pronyaev (Russia)
- 14:30 Variance analysis of the experimental data with prescribed statistical uncertainties, S. Badikov (Atomstandard, Russia)
- 15:00 Updating the $^{239}\text{Pu}(n,f)$ covariances in GMA with templates of expected uncertainties, D. Neudecker (LANL, USA)
- 15:25 Prototype of a new Bayesian evaluation system - development and validation, G. Schnabel (IAEA)

15:55 Break

- 16:05 Identifying physics reasons for outliers and systematic discrepancies in experimental $^{239}\text{Pu}(n,f)$ cross-section data using machine learning, D. Neudecker (LANL, USA)

16:30 Discussion

Friday, 16 October

14:00 Discussion (cont'd)

17:30 Closing of the meeting

APPENDIX II: PARTICIPANTS

Country	Name	Surname	Affiliation	Email
CHINA	Zhigang	GE	China Institute of Atomic Energy	gezg@ciae.ac.cn
	Xi	TAO	China Institute of Atomic Energy	taoxixishi@ciae.ac.cn
	Yuan	TIAN	China Institute of Atomic Energy	tiany@ciae.ac.cn
	Jimin	WANG	China Institute of Atomic Energy	jm wang@ciae.ac.cn
	Huang	XIAOLONG	China Institute of Atomic Energy	huang@ciae.ac.cn
	Ruirui	XU	China Institute of Atomic Energy	xrr-001@163.com
	Zhi	ZHANG	China Institute of Atomic Energy	zhangzhi479@ciae.ac.cn
	Zhenpeng	CHEN	Tsinghua University	zhpchen@mail.tsinghua.edu.cn
	Qianghua	WU	Tsinghua University	wuqh16@mails.tsinghua.edu.cn
FRANCE	Gilles	NOGUERE	Commissariat à l'énergie atomique et aux énergies alternatives	gilles.noguere@cea.fr
GERMANY	Ralf	NOLTE	Physikalisch-Technische Bundesanstalt	ralf.nolte@ptb.de
	Elisa	PIROVANO	Physikalisch-Technische Bundesanstalt	elisa.pirovano@ptb.de
	Rene	REIFARTH	Goethe-Universitaet Frankfurt	reifarth@physik.uni-frankfurt.de
	Stanislav	SIMAKOV	Karlsruher Institut fuer Technologie	stanislav.simakov@partner.kit.edu
	Anton	WALLNER	Helmholtz-Zentrum Dresden-Rossendorf	a.wallner@hzdr.de
ITALY	Simone	AMADUCCI	Istituto Nazionale die Fisica Nucleare	amaducci@lns.infn.it
	Luigi	COSENTINO	Istituto Nazionale die Fisica Nucleare	cosentino@lns.infn.it
	Paolo	FINOCCHIARO	Istituto Nazionale die Fisica Nucleare	finocchiaro@lns.infn.it
	Alice	MANNA	Istituto Nazionale die Fisica Nucleare	alice.manna@bo.infn.it
JAPAN	Osamu	IWAMOTO	Japan Atomic Energy Agency	iwamoto.osamu@jaea.go.jp
RUSSIA	Vladimir	PRONYAEV	Private	vgpronyaev@yandex.ru
SPAIN	Manuel	CAAMAÑO	Universidad de Santiago de Compostela	manuel.fresco@usc.es

Country	Name	Surname	Affiliation	Email
SPAIN cont'd	Ignacio	DURAN	Universidad de Santiago de Compostela	ignacio.duran@usc.es
	Javier	PRAENA	Universidad de Granada	jpnaena@ugr.es
UNITED STATES	Donald	SMITH	Private	donaldlarnedsmith@gmail.com
	Maria	ANASTASIOU	Lawrence Livermore National Laboratory	anastasiou2@llnl.gov
	Gregory	POTEL AGUILAR	Lawrence Livermore National Laboratory	potelaguilar1@llnl.gov
	Sofia	QUAGLIONI	Lawrence Livermore National Laboratory	quaglioni1@llnl.gov
	Anthony	RAMIREZ	Lawrence Livermore National Laboratory	ramirez112@llnl.gov
	Konstantinos	KRAVVARIS	Lawrence Livermore National Laboratory	kra vvaris1 @llnl.gov
	Lucas	SNYDER	Lawrence Livermore National Laboratory	snyder35@llnl.gov
	Denise	NEUDECKER	Los Alamos National Laboratory	dneudecker@lanl.gov
	Mark	PARIS	Los Alamos National Laboratory	m paris@lanl.gov
	Gerry	HALE	Los Alamos National Laboratory	ghale@lanl.gov
	Robert	McELROY	Oak Ridge National Laboratory	mcelroyrd@ornl.gov
	Allan	CARLSON	National Institute of Standards and Technology	carlson@nist.gov
	Hans Pieter	MUMM	National Institute of Standards and Technology	pieter@nist.gov
	Yaron	DANON	Rensselaer Polytechnic Institute	danony@rpi.edu
	Thomas	MASSEY	Ohio University	tnmassey56@gmail.com
Jeffrey	VANHOY	TUNL/Duke University & US Naval Academy	vanhoy@usna.edu	
INT. ORGANIZATION	Stefan	KOPECKY	European Commission, Joint Research Centre	stefan.kopecky@ec.europa.eu
	Peter	SCHILLEBEECKX	European Commission, Joint Research Centre	peter.schillebeeckx@ec.europa.eu
	Carlos	PARADELA	European Commission, Joint Research Centre	carlos.paradela-dobarro@ec.europa.eu
	Roberto	CAPOTE	International Atomic Energy Agency	r.capoteny@iaea.org
	Georg	SCHNABEL	International Atomic Energy Agency	g.schnabel@iaea.org
	Arjan	KONING	International Atomic Energy Agency	a.koning@iaea.org
	Naohiko	OTSUKA	International Atomic Energy Agency	n.otsuka@iaea.org

APPENDIX III: PRESENTATION LINKS

#	Presenting Author	Title	Link
1	A. Carlson	Recent work on neutron standards	PDF
2	Z. Chen	${}^6\text{Li}(n,t)$ R-matrix fit of the CSNS Back-n data with RAC code	PDF
3	P. Finocchiaro	${}^{235}\text{U}(n,f)$ cross section from thermal to 170 keV	PDF
4	G. Hale	Recent LANL work on reactions in the ${}^7\text{Li}$ system	PDF
5	M. Paris	EDA R-matrix evaluations of NN and ${}^{17}\text{O}$ systems	PDF
6	T.N. Massey	${}^{11}\text{B}$ Compound nucleus reactions: ${}^{10}\text{B}(n,Z)$ reactions	PDF
7	S. Simakov	Reference prompt discrete γ -ray production and high energy fission cross sections	PDF
8	E. Pirovano	Measurement of ${}^{235}\text{U}(n,f)$ relative to ${}^1\text{H}(n,n)$ in the energy range from 30 to 150 MeV at n_TOF	PDF
9	L. Snyder	Fission TPC cross section ratio results	PDF
10	P. Mumm	${}^6\text{Li}(n,t)$ and ${}^{235}\text{U}(n,f)$ sub-thermal measurements via an absolute cold neutron flux monitor	PDF
11	Y. Danon	RPI measurements that can help improve cross section standards	PDF
12	J. Vanhoy	Carbon scattering cross section	PDF
13	G. Noguere	Multigroup evaluation of the ${}^{235}\text{U}(n,f)$, ${}^{238}\text{U}(n,\gamma)$, ${}^{238}\text{U}(n,f)$ and ${}^{239}\text{Pu}(n,f)$ cross sections with the CONRAD code by using the GMA database : preliminary results	PDF
14	I. Duran	On the thermal and resonance integrals as standards for neutron induced fission on major actinides	PDF
15	R. Reifarth	Review of gold capture data	PDF
16	J. Praena	${}^{197}\text{Au}(n,\gamma)$ 30 keV Maxwellian: absolute integral measurements	PDF
17	P. Schillebeeckx	${}^{238}\text{U}(n,\gamma)$ and ${}^{197}\text{Au}(n,\gamma)$ cross sections	PDF
18	A. Wallner	Status on AMS experiments: (1) ${}^{235}\text{U}(n,\gamma)$ at thermal and sub-thermal energies, (2) systematic differences between AMS & TOF, and (3) ${}^{235}\text{U}$ -PFNS – the threshold reaction ${}^{27}\text{Al}(n,2n)$	PDF
19	V. Pronyaev	Ad hoc approach for construction of USU covariances for GMA fit	PDF
20	S. Badikov	Variance analysis of the experimental data with prescribed statistical uncertainties	PDF
21	D. Neudecker	Updating the ${}^{239}\text{Pu}(n,f)$ covariances in GMA with templates of expected uncertainties	PDF
22	G. Schnabel	Prototype of a new Bayesian evaluation system - development and validation	PDF
23	D. Neudecker	Identifying physics reasons for outliers and systematic discrepancies in experimental ${}^{239}\text{Pu}(n,f)$ cross-section data using machine learning	PDF

Nuclear Data Section
International Atomic Energy Agency
Vienna International Centre, P.O. Box 100
A-1400 Vienna, Austria

E-mail: nds.contact-point@iaea.org
Fax: (43-1) 26007
Telephone: (43-1) 2600 21725
Web: <http://nds.iaea.org>
